Hakula, Harri; Nasser, Mohamed M.S.; Vuorinen, Matti

Conformal capacity and polycircular domains

Published in:
Journal of Computational and Applied Mathematics

DOI:
10.1016/j.cam.2022.114802

Published: 01/03/2023

Document Version
Publisher's PDF, also known as Version of record

Journal of Computational and Applied Mathematics 420 (2023) 114802

Contents lists available at ScienceDirect

Journal of Computational and Applied Mathematics

journal homepage: www.elsevier.com/locate/cam

Conformal capacity and polycircular domains

Harri Hakula [a,*], Mohamed M.S. Nasser [b,c], Matti Vuorinen [d]

[a] Aalto University, Department of Mathematics and Systems Analysis, P.O. Box 11100, FI-00076 Aalto, Finland
[b] Department of Mathematics, Statistics, and Physics, Wichita State University, Wichita, KS 67260-0033, USA
[c] Department of Mathematics, Statistics, and Physics, Qatar University, Doha, Qatar
[d] Department of Mathematics and Statistics, University of Turku, FI-20014 Turku, Finland

ARTICLE INFO

Article history:
Received 28 February 2022
Received in revised form 1 July 2022

Keywords:
Multiply connected domains
Condenser capacity
Capacity computation

ABSTRACT

We study numerical conformal mapping of multiply connected planar domains with boundaries consisting of unions of finitely many circular arcs, so called polycircular domains. We compute the conformal capacities of condensers defined by polycircular domains. Experimental error estimates are provided for the computed capacity and, when possible, the rate of convergence under refinement of discretization is analyzed. The main ingredients of the computation are two computational methods, on one hand the boundary integral equation method combined with the fast multipole method and on the other hand the *hp*-FEM method. The results obtained with these two methods agree with high accuracy.

1. Introduction

During the past century, *domain functionals* of planar domains have been extensively studied in geometric function theory and other fields of mathematical analysis. Some of these functionals are harmonic measure, hyperbolic distance and its various generalizations, conformal radius, and various domain characteristics, for instance, uniform perfectness. One way to classify these notions is their invariance properties such as invariance under conformal mappings, Möbius transformations or stretchings. We study here one of these functionals, the conformal capacity of a condenser. A *condenser* is a pair (G, E) where $G \subset \mathbb{R}^2$ is a domain and $E \subset G$ is a non-empty compact set and the *conformal capacity* is defined as follows

$$\operatorname{cap}(G, E) = \inf_{u \in A} \int_G |\nabla u|^2 \, dm, \tag{1.1}$$

where A is the family of all harmonic functions u defined in G with $u(x) \geq 1$ for all $x \in E$ and $u(x) \to 0$ when $x \to \partial G$. In concrete applications the sets E and ∂G have a simple geometry, both have a finite number of components, each component being a piecewise smooth curve. In this paper we assume that G is a simply connected domain and the domain $G \setminus E$ is multiply connected and all of its boundary components are finite unions of circular arcs or linear segments. Such domains are known as *polycircular domains*. This term is due to D. Crowdy [1]. In this case, it is known that the infimum is attained by a harmonic function [2, p. 65], [3]. Moreover, this extremal function is a solution to the Dirichlet problem

$$\Delta u = 0, \quad \text{on } G \setminus E, \tag{1.2a}$$

$$u = 0, \quad \text{on } \partial G, \tag{1.2b}$$

* Corresponding author.
E-mail addresses: harri.hakula@aalto.fi (H. Hakula), mms.nasser@wichita.edu (M.M.S. Nasser), vuorinen@utu.fi (M. Vuorinen).

https://doi.org/10.1016/j.cam.2022.114802

$$u = 1, \quad \text{on } \partial E, \tag{1.2c}$$

and hence the capacity can be expressed in terms of this extremal function as

$$\operatorname{cap}(G, E) = \iint_{\Omega} |\nabla u|^2 \, dm \tag{1.3}$$

where $\Omega = G \setminus E$. Let $\Gamma_0 = \partial G$, $\partial E = \Gamma_1 \cup \cdots \cup \Gamma_m$, where Γ_0 encloses all the other curves $\Gamma_1, \ldots, \Gamma_m$. Then each of the boundary components Γ_j is a piecewise smooth Jordan curve with a finite number of corner points. We assume that none of these corner points is a cusp, that is, the boundary arcs meet at nonzero angles. The orientation of the total boundary $\Gamma = \partial\Omega = \Gamma_0 \cup \Gamma_1 \cup \cdots \cup \Gamma_m$ is assumed to be such that Ω is on the left of Γ. The above Dirichlet problem (1.2) in multiply connected domains is a wide area of research, see e.g. [4].

In their classical book G. Polya and G. Szegö [5] studied extensively various estimates for capacities in terms of various domain functionals, however their capacity was not the conformal capacity. V. Dubinin [3] studied conformal capacity in many function theoretic applications and the book of J. Garnett and D. Marshall [6] is an extensive treatise of harmonic measure and its applications to potential theory and geometric function theory.

In spite of their important role in geometric function theory, explicit formulas or numerical values of conformal invariants are known only in the simplest cases. Roughly speaking one can say that when the domain connectivity increases, the more difficult it is to find explicit formulas even for simple domains like the circular domains where all the boundary components are circles. The connectivity of $G \setminus E$ depends on the number of topological components of E and $G \setminus E$ is doubly connected if ∂E is a simple curve. Our goal here is to continue our earlier work [7–9] and to develop algorithms for the computation of $\operatorname{cap}(G, E)$. For an example, see Fig. 1 where $G = \mathbb{B}^2$ and $\mathbb{B}^2$ is the unit disk.

Numerical computation of conformal capacity has been studied in some earlier papers [8,9], but we have not seen any results for conformal capacities of condensers for multiply connected polycircular domains of the type described above. Due to the conformal invariance of the conformal capacity, an auxiliary step in the computation is often to apply conformal mappings onto a canonical domain to simplify the geometry [10]. For example, the conformal capacity for the doubly connected domain shown in Fig. 1 can be computed by finding the conformal mapping $w = f(z)$ from this domain onto an annulus domain $q < |w| < 1$ and hence the conformal capacity is $2\pi / \log(1/q)$. The books of N. Papamichael- N. Stylianopoulos [11] and P. Kythe [12] and the long survey of R. Wegmann [13] are valuable general sources, see also [11, pp. 14–16] for an overview of the literature. We will now review the most recent literature from the point of view of polycircular domains.

Conformal mapping of Jordan domains with the boundary consisting of a union of finitely many circular arcs, has been studied by P. Brown and M. Porter [14,15], by U. Bauer and W. Lauf [16], and, in particular, by D. Crowdy [1], D. Crowdy and A. Fokas [17], and by D. Crowdy, A. Fokas, and C. Green [17]. See also [18–20]. In [1,17,21], D. Crowdy and his coauthors developed an extensive theory based on Schottky's prime function method for the construction of conformal mappings from multiply connected circular domains onto polycircular arc domains. In the case of multiply connected polycircular domains, conformal mappings onto canonical domains have been investigated also in [22–26]. Several types of canonical domains are used as an intermediate step of computation. Some examples are those where the boundary components are circles or parallel slits or concentric circular arcs. M. Badreddine, T. DeLillo, and S. Sahraei [27] compare several numerical conformal mapping methods for multiply connected polycircular domains. Computer graphics applications of conformal mapping of multiply connected domains appear in [28]. The goal of our research here is different from the above references as our focus is on conformal capacity. For this purpose we apply two numerical methods, the *hp*-FEM and the method based on the Boundary Integral Equation (BIE) with the generalized Neumann kernel. Using these methods, our primary goal is to present detailed numerical reference results on capacities of multiply connected polycircular domains that have not been considered before. The secondary goal is to verify the correctness of the BIE method by taking the hp-FEM, a well-established standard method, as the reference and to compare the performance of these two methods.

The quantity of interest, the capacity of a condenser, is directly applicable in engineering contexts. Since the Dirichlet problem is one of the primary numerical model problems, any standard solution technique can be viewed as having been validated. In this paper, the novelty is the method of verification of the results. Instead of merely comparing different discretizations, we make use of *two different methods* to verify the correctness of the results. The first method is based on the BIE with the generalized Neumann kernel as developed and implemented in MATLAB in a series of papers during the past two decades, see e.g. [29]–[30]. The method uses the fast multipole method implementation from [31] for the speed-up of solving linear equations with a special structure. The BIE method has been used to solve several problems in domains of very high connectivity, domains with piecewise smooth boundaries, domains with close-to-touching boundaries, and in domains of real-world problems. In a recent series of papers [32]–[9], the method was applied for the capacity computation of planar condensers and for the analysis of isoperimetric problems for capacity. In particular, we will make use of the very recent results [8].

The second method, *hp*-FEM, is based on a Mathematica implementation developed and widely tested by H. Hakula during the past two decades, [33,34]. The method allows one to incorporate *a priori* knowledge of the singularities into highly non-quasiuniform meshes, within which the polynomial order can vary from element to element. In the class of problems discussed here, one would expect exponential convergence in the natural norm if the discretization is refined properly.

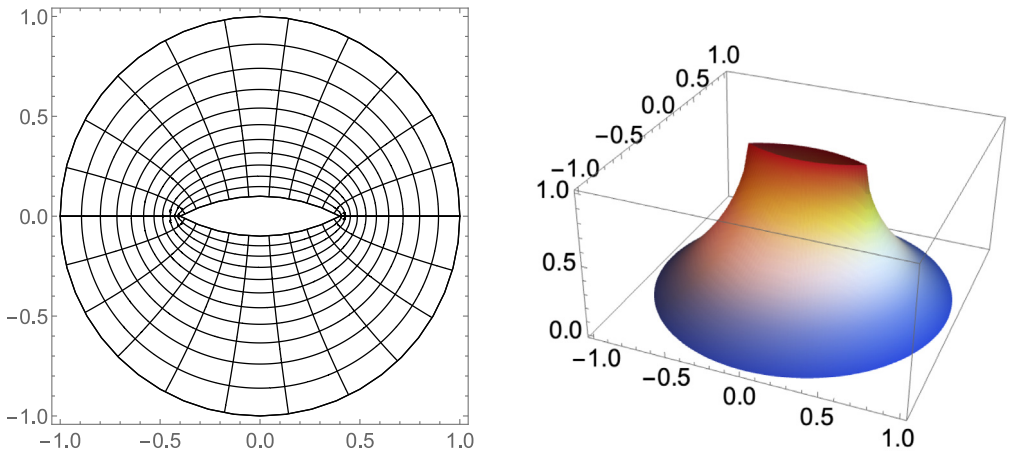

Fig. 1. A polycircular ring domain with the lens boundary ∂E is defined by two circular arcs passing through the points $(-r, 0), (0, \pm s), (r, 0)$, respectively. Here $r = 2/5$, $s = 1/10$. The capacity of this ring domain can be computed by computing a conformal map from this domain onto an annular domain. The left figure (a) shows the gridlines mapped onto a polar grid, consisting of radial segments and circles, under this map. The numerical value of the capacity given by the *hp*-FEM is $\mathrm{cap}(\mathbb{B}^2, E) = 4.371029672008615$. In (b) the potential function is illustrated.

The BIE method converges exponentially for analytic boundaries and algebraically for piecewise smooth boundaries, see e.g., [35]. However, so far, no numerical comparison with other methods has been made in the literature, especially for domains with corners. As mentioned above, one of the objectives of this paper is to present such a comparison where the BIE is compared against the *hp*-FEM. We obtain surprisingly good agreements between the two methods. The obtained results show that the BIE indeed gives accurate results for domains with corners even if the angles at the corners are small.

The structure of this paper is as follows. In Section 2, we introduce some notation and terminology. Section 3 is a short summary of the two methods we use, the *hp*-FEM and the boundary integral equation method. In Section 4 we compute the capacities of several multiply connected polycircular condensers and compare the performance of the methods. Moreover, the computational error is analyzed as a function of the number of degrees of freedom. Section 5 deals with condensers $(\mathbb{B}^2, E)$ where the compact set E has lens-shaped structure and we study how closely the theoretical Möbius invariance can be observed in numerical computations. Some concluding remarks are given in Section 6.

2. Preliminary notions

The capacity of a condenser defined in the introduction (1.1) can be defined in terms of the Dirichlet problem (1.2) as well as in many other equivalent ways as shown in [3,36]. First, the family A of functions in (1.1) may be replaced by several other families by [36, Lemma 5.21, p. 161]. Furthermore, the capacity is equal to the modulus of a curve family

$$\mathrm{cap}(G, E) = \mathsf{M}(\Delta(E, \partial G; G)), \tag{2.1}$$

where $\Delta(E, \partial G; G)$ is the family of all curves joining E with the boundary ∂G in the domain G and M stands for the modulus of a curve family [36, Thm 5.23, p. 164]. For the basic facts about capacities and moduli, the reader is referred to [3,36,37].

2.1. Quadrilaterals

A Jordan domain in the complex plane $\mathbb{C}$ is a domain with boundary homeomorphic to the unit circle. A *quadrilateral* is a Jordan domain D together with four distinguished points $z_1, z_2, z_3, z_4 \in \partial D$ which define a positive orientation of the boundary. In other words, if we traverse the boundary, then the points occur in the order of indices and the domain D is on the left-hand side. The quadrilateral is denoted by $(D; z_1, z_2, z_3, z_4)$. The *modulus of the quadrilateral* [11, p. 52] is a unique positive number h such that D can be conformally mapped by some conformal map f onto the rectangle with vertices $0, 1, 1 + \mathrm{i}h, \mathrm{i}h$ with

$$f(z_1) = 0, \quad f(z_2) = 1, \quad f(z_3) = 1 + \mathrm{i}h, \quad f(z_1) = \mathrm{i}h.$$

The modulus is denoted $\mathrm{mod}(D; z_1, z_2, z_3, z_4)$. The following basic formula is often used:

$$\mathrm{mod}(D; z_1, z_2, z_3, z_4)\,\mathrm{mod}(D; z_2, z_3, z_4, z_1) = 1\,. \tag{2.2}$$

A rectangle with sides a and b and its vertices define a quadrilateral. Depending on the labeling of its vertices, its modulus is either a/b or b/a. An alternative equivalent definition of the modulus of a quadrilateral is based on the mixed Dirichlet–Neumann problem by L.V. Ahlfors [2, Thm 4.5, p. 65].

2.2. Quadrilateral modulus and curve families

The modulus of a quadrilateral $(D; z_1, z_2, z_3, z_4)$ is connected with the modulus of the family of all curves in D, joining the opposite boundary arcs (z_2, z_3) and (z_4, z_1), in a very simple way, as follows

$$\operatorname{mod}(D; z_1, z_2, z_3, z_4) = \mathsf{M}(\Delta((z_2, z_3), (z_4, z_1); D)) . \tag{2.3}$$

Let $\operatorname{mod}_{\text{cal}}(D; z_1, z_2, z_3, z_4)$ be the computed approximate value to $\operatorname{mod}(D; z_1, z_2, z_3, z_4)$. Then, for every quadrilateral the so-called reciprocal relation (2.2) can be rephrased as an error estimate (Definition 2.4) which will be used below as one of our experimental error estimates.

Definition 2.4 (*Reciprocal Identity and Error*)**.** We shall call

$$\varepsilon_R = |1 - \operatorname{mod}_{\text{cal}}(D; z_1, z_2, z_3, z_4) \operatorname{mod}_{\text{cal}}(D; z_2, z_3, z_4, z_1)| \tag{2.5}$$

the error measure and

$$\varepsilon_N = \left| \lceil \log_{10} |\varepsilon_R| \rceil \right|$$

the related error number. This error characteristic was systematically used in [33,34] where it was shown to be usually compatible with other error characteristics.

3. Numerical methods used in computing capacities on polycircular domains

In this section the two methods used in this paper, the *hp*-FEM and the boundary integral equation (BIE) method, are introduced. Much of the material is standard, however, terminology and error concepts used in the discussion on numerical experiments is defined here.

3.1. High-order finite elements

The finite element method (FEM) is the standard numerical method for solving elliptic partial differential equations. Since FEM is an energy minimization method it is eminently suitable for problems involving Dirichlet energy. In the context of this paper where the focus is on domains with singularities at the vertices, the *hp*-FEM variant is the most efficient one [38,39]. With proper grading of the meshes, even with uniform polynomial order exponential convergence can be achieved, even in problems with strong corner singularities.

In this section we give a brief overview of the method and our implementation [33,40]. Of particular importance is the possibility to estimate the error in the computed quantity of interest. As noted above, in the absence of exact solutions, within the method itself we have the option of *a posteriori* error estimation [41].

The equality (1.3) shows that the capacity of a condenser is the Dirichlet integral, i.e., the H^1-seminorm of the potential u squared, or, the energy norm squared, a quantity of interest which is natural in the FEM setting.

3.1.1. Mesh refinement and exponential convergence

In the *h*-version the accuracy of the discretization is controlled by the sizes of the elements. The degrees of freedom are associated with the nodes of the mesh and the nodal shape functions induce a partition of unity.

The idea behind the *p*-version is to associate degrees of freedom to topological entities of the mesh and control accuracy via the polynomial order. The shape functions are based on suitable orthogonal polynomials and their supports reflect the related topological entity, nodes, edges, faces (in 3D), and interior of the elements.

For instance, on a triangle of order p, there are three nodal shape functions, $p - 1$ shapes on each edge, and $(p - 1)(p - 2)/2$ shapes in the interior. If only nodal shape functions are included, the *p*-version reduces to the classical *h*-version. The *hp*-version simply refers to combination of the two refinement strategies.

For the Dirichlet problem (1.2) it can be shown that if the mesh is graded appropriately the method converges exponentially in some general norm such as the H^1-seminorm. Moreover, due to the construction of shape functions, it is natural to have large curved elements in the mesh without significant increase in the discretization error. Since the number of elements can be kept relatively low given that additional refinement can always be added via elementwise polynomial degree, variation in the boundary can be addressed directly at the level of the boundary representation in some exact parametric form.

To fully realize the potential of the *p*-version, one has to grade the meshes properly and therefore we really use the *hp*-version here. In Fig. 2 the basic refinement strategy is illustrated. We start with an initial mesh, where the corners with singularities are *isolated*, that is, the subsequent refinements of their neighboring elements do not interfere with each other. Then the mesh is refined using successive applications of replacement rules.

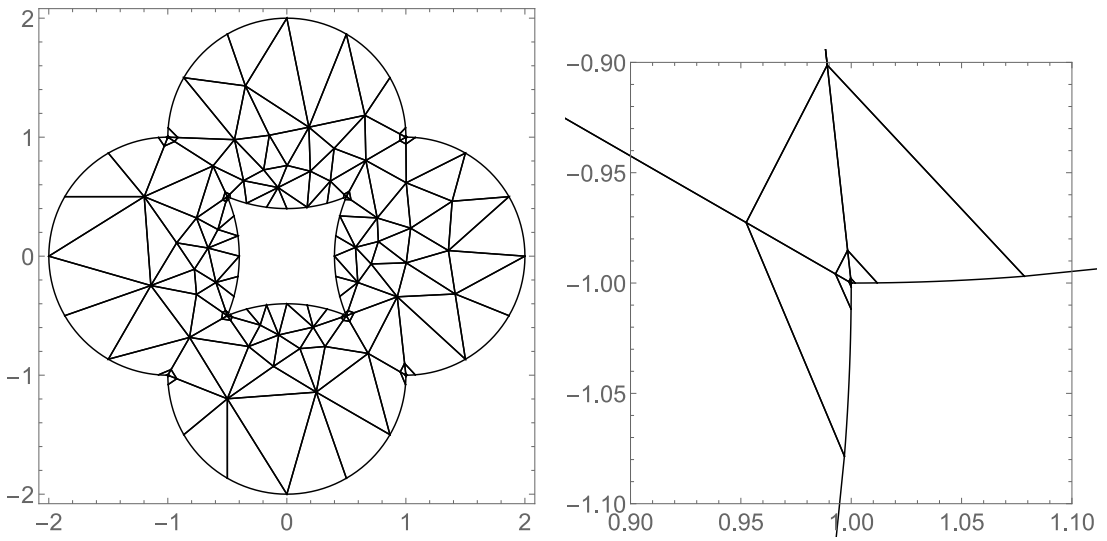

(a) After sixteen levels of refinement. (b) Mesh detail.

Fig. 2. Example of geometric grading of the mesh. We start with a coarse background triangulation. Once the singularities have been identified a priori, a sequence of geometric refinements is applied. Notice in (b) that the resulting mesh can include quadrilaterals and triangles. The high aspect ratios are compensated with high order polynomial basis.

In our implementation the geometry can be described in exact arithmetic and therefore there are not any fixed limits on the number of refinement levels. In the case of graded meshes one has to resolve the question of how to set the polynomial degrees at every element, indeed, a form of refinement of its own. One option in the case of strong singularities is to set the polynomial degree based on graph distance from the singularity. Here, however, the degree p is kept constant over the whole mesh despite the grading.

The following theorem due to Babuška and Guo [42] sets the limit to the rate of convergence. Notice that construction of appropriate spaces is technical. For rigorous treatment of the theory involved see Schwab [39] and references therein. For the Dirichlet problem (1.2) the following theorem relates the convergence of the capacity (or energy) and the number of degrees of freedom N.

Theorem 3.1. *Let $\Omega \subset \mathbb{R}^2$ be a polygon, v the FEM-solution of (1.2), and let the weak solution u_0 be in a suitable countably normed space where the derivatives of arbitrarily high order are controlled. Then*

$$\inf_v \|u_0 - v\|_{H^1(\Omega)} \leq C \ \exp(-b\sqrt[3]{N}),$$

where C and b are independent of N, the number of degrees of freedom. Here v is computed on a proper geometric mesh, where the order of an individual element is set to be its element graph distance to the nearest singularity. (The result also holds for meshes with constant polynomial degree.)

3.1.2. Error estimation: Reciprocal error and auxiliary space error estimate

Assuming that the exact capacity is not known, we have two types of error estimates available: the reciprocal estimate and an a posteriori estimate. Naturally, if the exact value is known, we can measure the true error.

The reciprocal error estimate introduced in Section 2 is rather unusual in the sense that even if this estimate is small, the calculation could still be far off – i.e. a small reciprocal error is a necessary but not sufficient condition for a small capacity error. In the context of this paper, the reciprocal error estimator (2.5) is useful in cases where the original problem can be reduced to one on a quadrilateral, for instance, using symmetries.

Our a posteriori error estimator of choice, the auxiliary space error estimate, belongs to a family of hierarchical error estimators. It is eminently suited to be used in conjunction of *hp*-FEM. Consider the abstract problem setting with u defined on the standard piecewise polynomial finite element space on some discretization T of the computational domain D. Assuming that the exact solution $u \in H_0^1(D)$ has finite energy, we arrive at the approximation problem: Find $\hat{u} \in V$ such that

$$a(\hat{u}, v) = l(v) \, (= a(u, v)) \quad (\forall v \in V), \tag{3.2}$$

where $a(\,\cdot\,,\,\cdot\,)$ and $l(\,\cdot\,)$, are the bilinear form and the load potential, respectively. Additional degrees of freedom can be introduced by enriching the space V. This is accomplished via introduction of an auxiliary subspace or "error space"

$W \subset H_0^1(D)$ such that $V \cap W = \{0\}$. We can then define the error problem: Find $\varepsilon \in W$ such that

$$a(\varepsilon, v) = l(v) - a(\hat{u}, v) (= a(u - \hat{u}, v)) \quad (\forall v \in W). \tag{3.3}$$

This is simply a projection of the residual to the auxiliary space. In 2D the space W, that is, the additional unknowns, can be associated with element edges and interiors. Thus, as mentioned above, for *hp*-methods this kind of error estimation is natural. The main result on this kind of estimators for the Dirichlet problem (1.2) is the following theorem.

Theorem 3.4 ([41]). *There is a constant K depending only on the dimension d, polynomial degree p, continuity and coercivity constants C and c, and the shape-regularity of the triangulation $\mathcal{T}$ such that*

$$\frac{c}{C} \|\varepsilon\|_1 \le \|u - \hat{u}\|_1 \le K \left(\|\varepsilon\|_1 + \operatorname{osc}(R, r, \mathcal{T})\right),$$

where the residual oscillation depends on the volumetric and face residuals R and r, and the triangulation $\mathcal{T}$.

The solution ε of (3.3) is called the *error function*. It has many useful properties for both theoretical and practical considerations. In particular, the error function can be numerically evaluated and analyzed for any finite element solution. By construction, the error function is always zero at the mesh points. In the examples below, the space W contains edge shape functions of degree $p + 1$ and internal shape functions of degrees $p + 1$ and $p + 2$. This choice is not arbitrary but based on careful cost analysis [41].

A key measure of the quality of the estimator is its effectivity in a norm of interest, here we define the effectivity index λ as follows:

$$\lambda = \|u - \hat{u}\|_1 / \|\varepsilon\|_1. \tag{3.5}$$

3.2. The boundary integral equation method

Using Green's formula [3, p. 4], and in view of (1.2b)–(1.2c), formula (1.3) can be written as

$$\operatorname{cap}(C) = \int_\Gamma u \frac{\partial u}{\partial \mathbf{n}} ds = \sum_{k=1}^{m} \int_{\Gamma_k} \frac{\partial u}{\partial \mathbf{n}} ds. \tag{3.6}$$

Further, the harmonic function u is the real part of an analytic function F in G which is not necessarily single-valued. Assume for each $k = 1, 2, \ldots, m$ that α_k is an auxiliary point enclosed by Γ_k. Then the function F can be written as [6,43,44]

$$F(z) = g(z) - \sum_{k=1}^{m} a_k \log(z - \alpha_k) \tag{3.7}$$

where g is a single-valued analytic function in G and $a_1, \ldots, a_m$ are undetermined real constants such that [44, §31]

$$a_k = \frac{1}{2\pi} \int_{\Gamma_k} \frac{\partial u}{\partial \mathbf{n}} ds, \quad k = 1, 2, \ldots, m. \tag{3.8}$$

Thus, it follows from (3.6) that

$$\operatorname{cap}(C) = 2\pi \sum_{k=1}^{m} a_k. \tag{3.9}$$

See [8] for more details.

The problem (1.2) above is a particular case of the problem considered in [8, Eq. (4)]. So, the constants $a_1, \ldots, a_m$ in (3.9) can be computed using the BIE method presented in [8, Theorem 4] which is based on using the BIE with the generalized Neumann kernel. For domains with smooth boundaries, the BIE can be solved accurately using the Nyström method with equidistant trapezoidal rule. For smooth boundaries of class C^{q+2} and smooth integrand of class C^q, the trapezoidal Nyström method converges with order $O(1/n^q)$ where n is the number of mesh points [45]. A MATLAB function `fbie` for solving the BIE with the generalized Neumann using the trapezoidal Nyström method is presented in [35] and this function will be used in this paper. However, in this paper, we consider polycircular domains. For such domains, the solution of the BIE has a singularity in its derivative in the vicinity of the corner points [46, p. 390] and this causes that the equidistant trapezoidal rule yields only poor convergence [45]. To achieve a satisfactory accuracy, we discretize the BIE using a graded mesh and then applying the Nyström's method [45–47]. To describe such a graded mesh method, we assume that the boundary component Γ_j consists of ℓ circular arcs or segments, then Γ_j has ℓ corner points. We first parametrize each boundary component Γ_j by a 2π-periodic function $\zeta_j(t)$ for $t \in J_j = [0, 2\pi]$. The function $\zeta_j(t)$ is assumed to be smooth with $\zeta_j'(t) \neq 0$ for all values of $t \in J_j$ such that $\zeta_j(t)$ is not a corner point. We assume that $\zeta_j'(t)$ has only the first kind discontinuity at these corner points. If $\zeta_j(\hat{t})$ is a corner point, we define $\zeta_j'(\hat{t}) := \zeta_j'(\hat{t} - 0)$. Let J be the disjoint

union of the $m+1$ intervals $J_j = [0, 2\pi]$, $j = 0, 1, \ldots, m$. We define a parametrization of the whole boundary Γ on J by (see [35] for the details)

$$\zeta(t) = \begin{cases} \zeta_0(t), & t \in J_0, \\ \zeta_1(t), & t \in J_1, \\ \quad \vdots & \\ \zeta_m(t), & t \in J_m. \end{cases}$$

Then, as noted in the first paragraph in [47], using the graded mesh method suggested in [45] for discretizing the BIE is equivalent to parameterizing the boundary Γ by

$$\eta(t) = \zeta(\delta(t)),$$

where the function $\delta(t)$ is defined in [48, pp. 696–697] which is chosen to remove the discontinuity in the derivatives of the solution of the BIE. Then, the BIE can be solved using the MATLAB function `fbie` as in the case of smooth domains.

With the parametrization $\eta(t)$ of the whole boundary Γ, we define a complex function A by

$$A(t) = \eta(t) - \alpha, \tag{3.10}$$

where α is a given point in the domain Ω. The generalized Neumann kernel $N(s,t)$ is defined for $(s,t) \in J \times J$ by

$$N(s,t) := \frac{1}{\pi} \operatorname{Im}\left(\frac{A(s)}{A(t)} \frac{\eta'(t)}{\eta(t) - \eta(s)}\right). \tag{3.11}$$

We define also the following kernel

$$M(s,t) := \frac{1}{\pi} \operatorname{Re}\left(\frac{A(s)}{A(t)} \frac{\eta'(t)}{\eta(t) - \eta(s)}\right), \quad (s,t) \in J \times J. \tag{3.12}$$

The kernel $N(s,t)$ is continuous and the kernel $M(s,t)$ is singular where the singular part involves the cotangent function. Hence, the integral operator $\mathbf{N}$ with the kernel $N(s,t)$ is compact and the integral operator $\mathbf{M}$ with the kernel $M(s,t)$ is singular. Further details can be found in [49].

The next theorem follows from [8, Theorem 4].

Theorem 3.13. *For each $k = 1, 2, \ldots, m$, let the function γ_k be defined by*

$$\gamma_k(t) = \log|\eta(t) - \alpha_k|, \tag{3.14}$$

let μ_k be the unique solution of the integral equation

$$\mu_k - \mathbf{N}\mu_k = -\mathbf{M}\gamma_k, \tag{3.15}$$

and let the piecewise constant function $h_k = (h_{0,k}, h_{1,k}, \ldots, h_{m,k})$ be given by

$$h_k = [\mathbf{M}\mu_k - (\mathbf{I} - \mathbf{N})\gamma_k]/2. \tag{3.16}$$

Then, the $m+1$ real constants $a_1, \ldots, a_m, c$ are the unique solution of the linear system

$$\begin{bmatrix} h_{0,1} & h_{0,2} & \cdots & h_{0,m} & 1 \\ h_{1,1} & h_{1,2} & \cdots & h_{1,m} & 1 \\ \vdots & \vdots & \ddots & \vdots & \vdots \\ h_{m,1} & h_{m,2} & \cdots & h_{m,m} & 1 \end{bmatrix} \begin{bmatrix} a_1 \\ a_2 \\ \vdots \\ a_m \\ c \end{bmatrix} = \begin{bmatrix} 0 \\ 1 \\ \vdots \\ 1 \end{bmatrix}. \tag{3.17}$$

Note that the function $h_k = (h_{0,k}, h_{1,k}, \ldots, h_{m,k})$ in (3.16) is a piecewise constant function, i.e., for $k = 1, \ldots, m$ and $p = 0, 1, \ldots, m$, the function h_k is constant on each boundary component Γ_p and the real constant $h_{p,k}$ is the value of h_k on Γ_p. For each $k = 1, 2, \ldots, m$, the solution μ_k of the BIE (3.15) and the piecewise constant function h_k in (3.16) will be computed using the MATLAB `fbie` from [35] by calling

```
[muk, hk] = fbie(et, etp, A, gamk, n, iprec, restart, gmrestol, maxit)
```

where `et` and `etp` are the discretization vectors of the parametrization $\eta(t)$ of the boundary Γ and its derivative. Here, n is the number of mesh points on each boundary component Γ_k, and hence the total number of mesh points on the whole boundary Γ is $(m+1)n$. The vectors `et` and `etp` are computed by the MATLAB function `cirarcp3pt` which is based on the above described method for parameterizing the boundary Γ and is available in https://github.com/mmsnasser/polycircular. Then the discretization vectors `A` and `gamk` of the functions $A(t)$ and $\gamma_k(t)$ are computed by (3.10) and (3.14), respectively.

By computing approximate values of the piecewise constant function $h_k = (h_{0,k}, h_{1,k}, \ldots, h_{m,k})$ in (3.16), we obtain the entries of the coefficient matrix of the $(m+1) \times (m+1)$ linear system (3.17). Since $m+1$ is the number of boundary

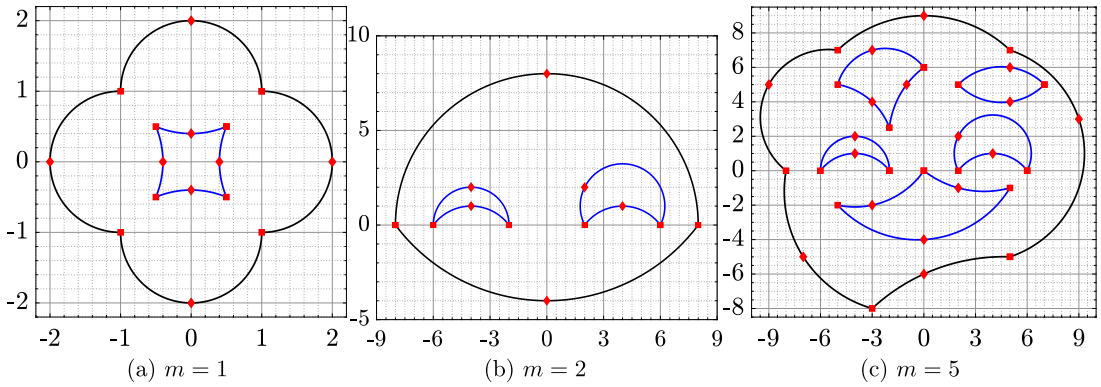

Fig. 3. Multiply connected polycircular domains. The number m refers to the number of interior components.

Table 1
The values of cap Ω for the multiply connected polycircular domains in Fig. 3. For $m = 1$ the computed reference value is 5.597545663702171. Agreement is taken to be the difference between the respective values.

	BIE Method		*hp*-FEM		Agreement
	Capacity	Time (s)	Capacity	Time (s)	
$m = 1$	5.597545657473350	2.518	5.597545663702324	19.56	6.23×10^{-9}
$m = 2$	10.95831566112476	5.206	10.95831564100293	12.18	6.52×10^{-9}
$m = 5$	21.25386110000110	25.29	21.25386107560764	69.48	2.44×10^{-8}

components of the domain $\Omega = G \setminus E$, we can assume that m is small (say, $m < 1000$). Hence, the linear system (3.17) will be solved using the Gauss elimination method. By solving the linear system, we obtain the values of the real constants $a_1, \ldots, a_m$ and hence the capacity $\mathrm{cap}(G, E)$ will be computed by (3.9).

The MATLAB function `fbie` is based on using the trapezoidal Nyström method. Thus, with the above parametrization $\eta(t)$ of the boundary Γ, it follows from [45, Theorems 2.1 and 4.4] that the order of the method is $Cn^{-(2q+1)}$ where q is an integer such that $2q + 1 \leq \hat{\alpha}p$ where $0 < \hat{\alpha} < 1$ and the constant C depends on $\hat{\alpha}$, q, and the integrand. The constant $\hat{\alpha}$ depends on the integrand which in turns depends on the parametrization $\eta(t)$ (see [45, Section 2] for more details). Here p is an integer known as the grading parameter and $p \geq 2$. It is involved in the definition of the function $\delta(t)$ (see [48, pp. 696–697]). Theoretically, choosing large values of p would increase the order of convergence of the method. However, choosing large value of p means that more grid points will be close to corner points which could cause some of these grids to be numerically equal for large values of n (in double precision calculations). In this paper, we choose $p = 3$ which suggests that the accuracy of the method is at best Cn^{-1}. However, the numerical results presented below in Fig. 7 illustrate that the order of the convergence of the method is better than Cn^{-1}.

Finally, a MATLAB function `capm` for computing the capacity using the above described method is given in https://github.com/mmsnasser/polycircular.

4. Verification experiments on polycircular domains

In this section, we consider three polycircular domains with $m = 1$, $m = 2$, and $m = 5$ (see Fig. 3). Each arc is determined by three points, two end points (squares) and one interior point (diamond). The purpose of these experiments is to establish the convergence rates of the methods and their respective accuracies using both error estimators and direct comparisons. The obtained approximate values of capΩ for both methods are shown in Table 1. The reported solution times indicate that BIE is generally faster. Whereas the times of BIE depend on the number of mesh points on each boundary component, on FEM the dependence is on the number of elements and the chosen polynomial order. Moreover, the timings do not reflect the time spent specifying the geometry, which for FEM can often be the dominant cost measured in time.

For the polycircular domain with $m = 1$ shown in Fig. 3(a), even though the exact reference capacity is not known, the domain is such that its inherent symmetries can be exploited. Consider a quarter domain $\Omega_{1/4}$ formed by connecting the opposing inner and outer arcs with straight edges (see the domain of Fig. 4(c)). Now we define the capacity of the quadrilateral $\Omega_{1/4}$ as in (1.2) except we add zero Neumann conditions on the straight edges. Using the reciprocal error estimator we can find with high confidence a numerical approximation which is close to machine precision. Interestingly, the auxiliary space error estimator agrees with the reciprocal error estimator (see Figs. 4(a) and 4(b)). For the quarter domain (see Figs. 4(c)–4(e)) we get

$$\mathrm{cap}\, \Omega_{1/4} = 1.399386415925543 \tag{4.1}$$

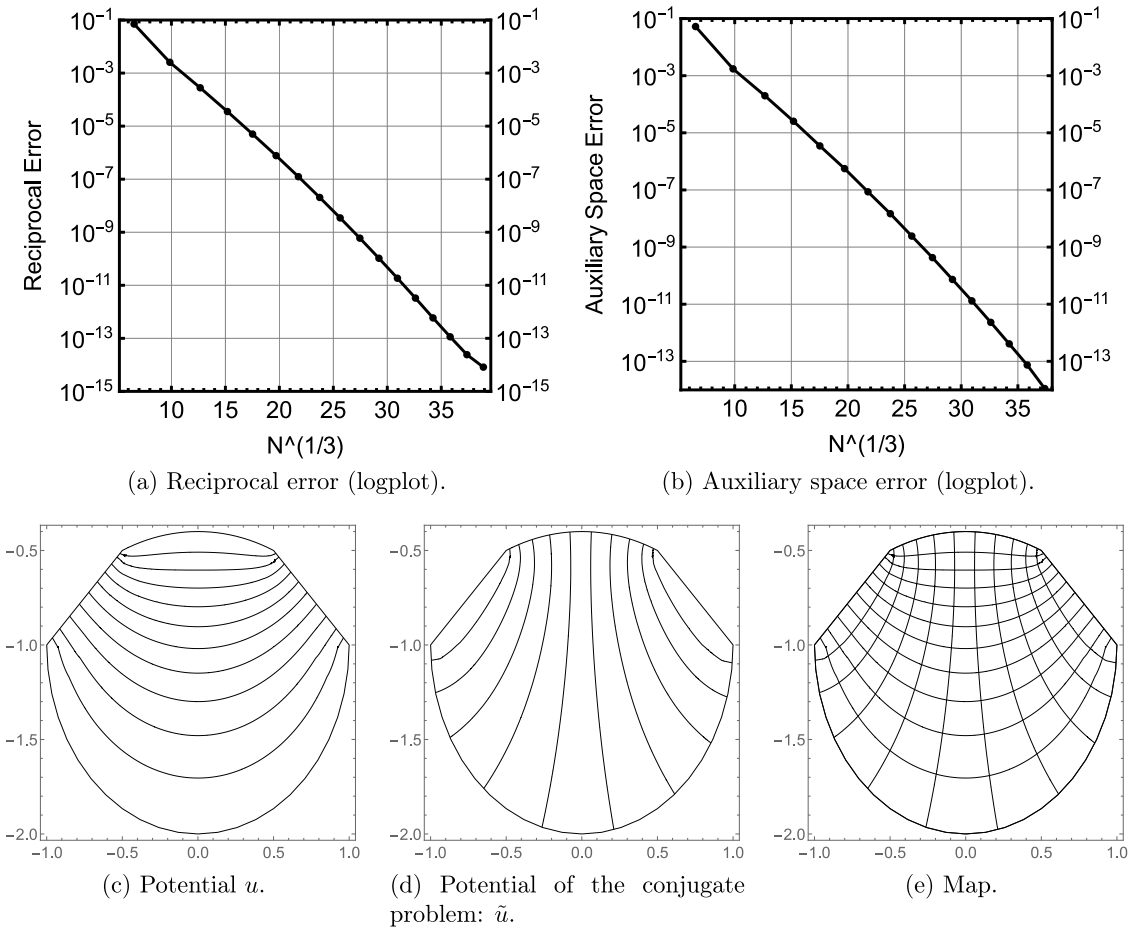

(a) Reciprocal error (logplot). (b) Auxiliary space error (logplot).

(c) Potential u. (d) Potential of the conjugate problem: $\tilde{u}$. (e) Map.

Fig. 4. Reference capacity via symmetry: $\Omega_{1/4}$. Two error estimates are given in (a) and (b), with error as function of $\sqrt[3]{N}$, where N is the number of degrees of freedom. In both cases the convergence is exponential as predicted by theory.

and thus the reference value

$$\operatorname{cap}\Omega = 4\operatorname{cap}\Omega_{1/4} = 5.597545663702171. \tag{4.2}$$

Using the reference value we can estimate the true error of the solution of the full discretization (see Fig. 5). For the *hp*-FEM, the convergence graph is given in Fig. 6(a). We get

$$\operatorname{cap}\Omega = 5.597545663702324, \tag{4.3}$$

and observe the error number $=$ 12 (13 significant digits). Again, the auxiliary space error estimator agrees with the effectivity index $\lambda_{m=1} \in [1.14, 1.38]$. For the other cases $\lambda_{m=2} \in [0.91, 1.40]$ and $\lambda_{m=5} \in [1.10, 1.37]$.

For the BIE method, the capacity capΩ is computed using the MATLAB function `capm`. We use $n = 2^{13}$ and $\alpha = \mathrm{i}$ for $m = 1$, $n = 2^{13}$ and $\alpha = 4\mathrm{i}$ for $m = 2$, and $n = 15 \times 2^9$ and $\alpha = 2\mathrm{i}$ for $m = 5$. For $m = 1$, the absolute value of the differences between the approximate values and the reference value in (4.2) vs. n are given in Fig. 7(a). As we can see from Fig. 7(a), the error is $O(n^{-2.73})$. For $m = 2$ and $m = 5$, the absolute error is computed by taking the values obtained by *hp*-FEM and presented in Table 1 as reference values. The errors are presented in Figs. 7(b)–7(c) which are $O(n^{-2.65})$ and $O(n^{-2.63})$, respectively. The presented results illustrate that the BIE method achieves a comparable level of accuracy with the *hp*-FEM.

5. Numerical experiments on domains with challenging boundaries

In this section we study three different aspects of polycircular domains. First, in the absence of exact capacity values, we study Möbius invariance of a given configuration. Here again, we can employ symmetries and obtain a numerical reference value of high accuracy. Second, we consider a domain with a jagged boundary with small angles, an interesting test case for BIE. Finally, a parameter-dependent configuration with lens-shaped boundary is tested against upper and lower bounds given in the literature. Also in this case symmetries can be exploited.

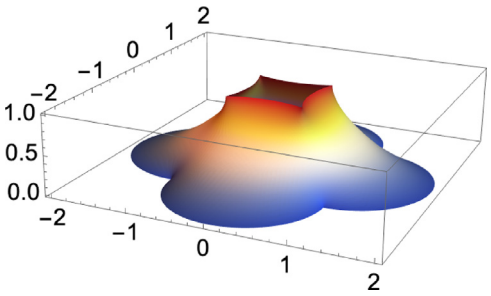

Fig. 5. Potential: $m = 1$.

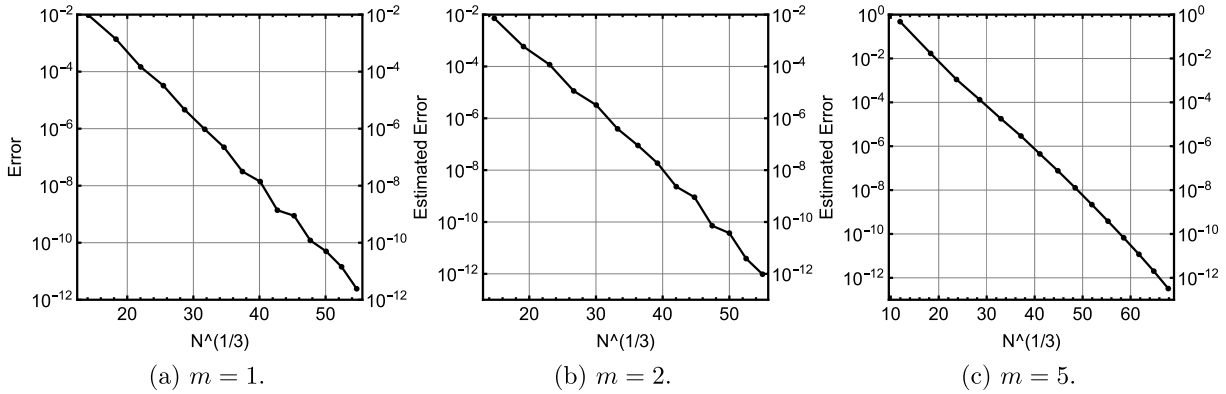

(a) $m = 1$. (b) $m = 2$. (c) $m = 5$.

Fig. 6. Error estimates (*hp*-FEM). Logplots with error as function of $\sqrt[3]{N}$. For $m = 1$ the reference value is computed using symmetries, in the other two cases, the last results in the *hp*-sequence is taken to be the reference. In all cases the obtained convergence is exponential with almost identical rate. The auxiliary error estimates coincide with the estimated errors and hence are not shown in the graphs. The similarity of the graphs gives us confidence in the choice of the reference values for the cases $m = 2$ and $m = 5$.

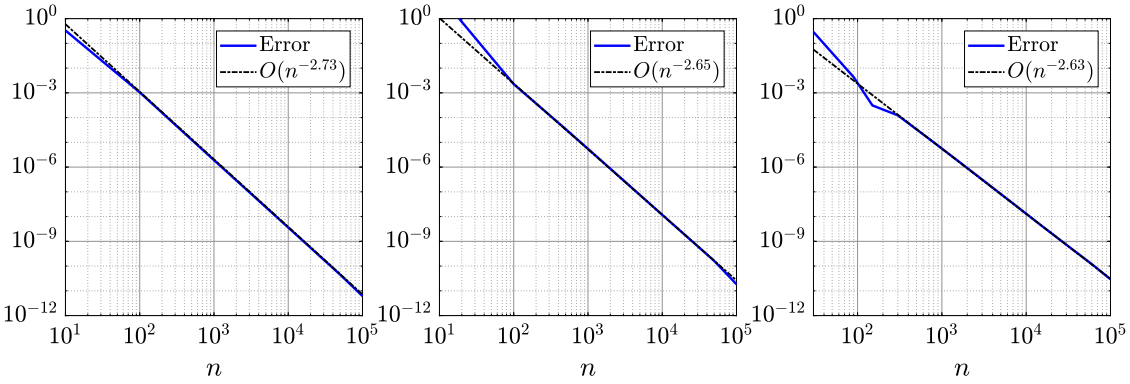

(a) $m = 1$. (b) $m = 2$. (c) $m = 5$.

Fig. 7. Error estimates (BIE). The error compared with the reference value in (4.2) for $m = 1$. For $m = 2$ and $m = 5$, the error is computed by taking the values obtained by *hp*-FEM and presented in Table 1 as reference values.

5.1. Checking the Möbius invariance

Unfortunately finding examples of polycircular condensers with known capacity looks too difficult. Therefore, one way to check the accuracy of the presented methods is to use the fact that capacity is conformal invariant. Consider the condenser $(\mathbb{B}^2, E)$ where E is the closure of the domain bordered by the circular arc polygon consists of two circular arcs, the first one passes through the three points -2, 0.6i, and 0.2, and the second one passes through the points 0.2, 0.1i, and -0.2 (see Fig. 8). Let

$$T_a(z) = \frac{z - a}{1 - \bar{a}z}$$

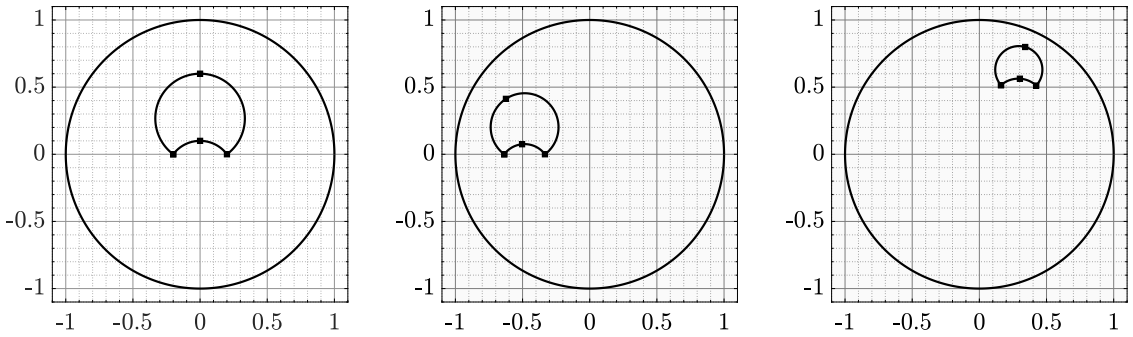

Fig. 8. The condenser $(\mathbb{B}^2, E)$ (left) and the condenser $(\mathbb{B}^2, T_a(E))$ for $a = 0.5$ (center), and $a = -0.3 - 0.5\mathrm{i}$ (right).

Table 2
The approximate values $\mathrm{cap}(\mathbb{B}^2, T_a(E))$ and the error $\left|\mathrm{cap}(\mathbb{B}^2, E) - \mathrm{cap}(\mathbb{B}^2, T_a(E))\right|$ where $\mathrm{cap}(\mathbb{B}^2, E) = \mathrm{cap}(\mathbb{B}^2, T_0(E))$. The two methods agree with 10 significant digits. The reference value for $a = 0$ is 6.044918141954128.

a	BIE Method		*hp*-FEM	
	$\mathrm{cap}(\mathbb{B}^2, T_a(E))$	Error	$\mathrm{cap}(\mathbb{B}^2, T_a(E))$	Error
0	6.04491814238562	–	6.044918141954396	–
0.1	6.04491814238563	9.77×10^{-15}	6.044918141954359	3.73×10^{-14}
0.5	6.04491814238567	4.88×10^{-14}	6.044918141954392	3.55×10^{-15}
$0.1 + 0.3\mathrm{i}$	6.04491814238559	2.93×10^{-14}	6.044918141954345	5.06×10^{-14}
$-0.2 + 0.5\mathrm{i}$	6.04491814238574	1.18×10^{-13}	6.044918141954328	6.75×10^{-14}
$-0.3 - 0.5\mathrm{i}$	6.04491814238566	3.55×10^{-14}	6.044918141954332	6.39×10^{-14}

be a Möbius transformation where $a \in \mathbb{B}^2$. Then, by the conformal invariance of the capacity, we should have

$$\mathrm{cap}(\mathbb{B}^2, E) = \mathrm{cap}(\mathbb{B}^2, T_a(E)).$$

The two numerical methods are used to compute $\mathrm{cap}(\mathbb{B}^2, T_a(E))$ for several values of a and

$$\left|\mathrm{cap}(\mathbb{B}^2, E) - \mathrm{cap}(\mathbb{B}^2, T_a(E))\right|$$

is considered to be the error in the computed values. The obtained results are presented in Table 2 for several values of a where $T_0(E) = E$. For the BIE method, we use $n = 2^{12}$, $\alpha = T_a(-0.3\mathrm{i})$, and $\alpha_1 = T_a(0.3\mathrm{i})$. Both methods, the BIE method and the *hp*-FEM, give results with almost the same level of high accuracy.

5.2. Bart Simpson condenser

We assume that E has a Bart Simpson shape as shown in Fig. 9. The vertices of the E are $3/9 + \mathrm{i}/9$, $3/9 - 3\mathrm{i}/9$, $-3/9 - 3\mathrm{i}/9$, $-3/9 + \mathrm{i}/9$, $4\mathrm{i}/9$, $-1/9 + \mathrm{i}/9$, $2/9 + 4\mathrm{i}/9$, $1/9 + \mathrm{i}/9$, and $4/9 + 4\mathrm{i}/9$. The arcs in Fig. 9 are determined either by their end-points and a point on each arc, which are $-2/9 + 3\mathrm{i}/9$, $3\mathrm{i}/9$, $2/9 + 3\mathrm{i}/9$, respectively, or by their end-points and the center of the circle containing the arc, which are $4/9 + \mathrm{i}/9$, $6/9 + \mathrm{i}/9$, and $8/9 + \mathrm{i}/9$, respectively. Note that the inner boundary has no cusps as the outer angles at the vertices $-1/9 + \mathrm{i}/9$ and $1/9 + \mathrm{i}/9$ are approximately 8°.

Here the capacity obtained with *hp*-FEM with $p = 18$ is $\mathrm{cap}(\mathbb{B}^2, E) = 7.265682491066263$ and the corresponding error estimate is $\sim 10^{-8}$. The BIE method used with $n = 9 \times 2^{11}$, $\alpha = -0.5\mathrm{i}$, and $\alpha_1 = 0$ gives the approximate value $\mathrm{cap}(\mathbb{B}^2, E) = 7.26568246621964$ which agrees with eight significant digits with the approximate value obtained by the FEM method. The difference between the two results is within the auxiliary space error estimate. Further, the approximate values for $\mathrm{cap}(\mathbb{B}^2, E)$ obtained for several values of n are given in the table in Fig. 9(b). These presented results demonstrate that the BIE method gives accurate results even though the angles of two corner points are small (approximately equal 8°).

5.3. Lens domains

Consider the condenser $(\mathbb{D}, E)$ where E is the closure of the lens domain bordered by the two circular arcs, the first one passes through the points $r, -\mathrm{i}s, -r$, and the second one passes through the points $-r, \mathrm{i}s, r$ (see Fig. 10a for $r = 0.8$ and $s = 0.3$). The BIE method is used to compute the capacity of the condenser $(\mathbb{D}, E)$ for $r = 0.8$ and for $0.05 \le s \le r$. The obtained results are shown in Fig. 11. The convergence graph for a single instance $r = 0.8$ and $s = 0.3$ is shown in

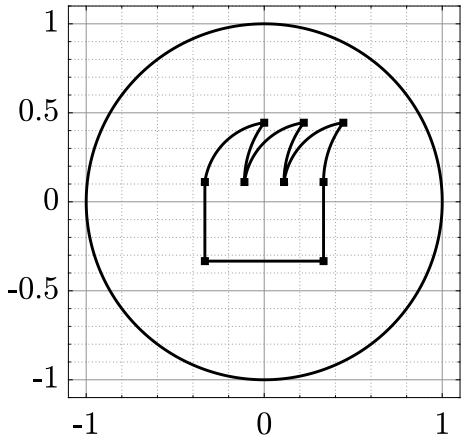

(a) The domain.

n	$\mathrm{cap}(\mathbb{B}^2, E)$
9×2^8	7.26568934865634
9×2^9	7.26568351878449
9×2^{10}	7.26568260732833
9×2^{11}	7.26568246621964

(b) BIE convergence.

Fig. 9. Bart Simpson condenser. The domain and capacities computed with BIE.

Fig. 10b. The values of the capacity $\mathrm{cap}(\mathbb{D}, E)$ vs. the hyperbolic perimeter of E, $L = \text{hyp-perim}(E)$, are presented in Fig. 11. It is known that [32, Eqs (5.13)–(5.15)]

$$\frac{2\pi}{\log\left(\sqrt{1+(2\pi/L)^2}+2\pi/L\right)} \tag{5.1}$$

is an upper bound for $\mathrm{cap}(\mathbb{D}, E)$ and, since E is convex,

$$\frac{2\pi}{\mu\left(\mathrm{th}(L/4)\right)} \tag{5.2}$$

is a lower bound for $\mathrm{cap}(\mathbb{D}, E)$, where [37, p. 122]

$$\mu(r) = \frac{\pi}{2}\frac{\mathcal{K}'(r)}{\mathcal{K}(r)}, \quad \mathcal{K}(r) = \int_0^1 \frac{dx}{\sqrt{(1-x^2)(1-r^2x^2)}}, \quad \mathcal{K}'(r) = \mathcal{K}(r'), \quad r' = \sqrt{1-r^2}\,. \tag{5.3}$$

Here, $\mathcal{K}(r)$ and $\mathcal{K}'(r)$ are the complete elliptic integrals of the first kind. These bounds are shown in Fig. 11 as well.

Note that for $s = r = 0.8$, the set E is the closed disk $\overline{B(0,r)} = \{z : |z| \le r\}$ and the capacity $\mathrm{cap}(\mathbb{D}, E)$ for the latter case is $2\pi/\log(1/r)$ and hence, for $r = 0.8$, equal to 28.157593038985901 which is the horizontal dotted-line in Fig. 11. In the case $s = 0$, the set $E = [-r, r]$, and hence, by the Möbius transform

$$z \mapsto \frac{z+r}{1+rz},$$

the domain $\mathbb{D}\backslash E$ is mapped to the domain $\mathbb{D}\backslash\hat{E}$ where $\hat{E} = [0, 2r/(1+r^2)]$. Hence,

$$\mathrm{cap}(\mathbb{D}, E) = \mathrm{cap}(\mathbb{D}, \hat{E}) = \frac{2\pi}{\mu\left(\frac{2r}{1+r^2}\right)}$$

and we see that for $r = 0.8$, $\mathrm{cap}(\mathbb{D}, E) = 7.360222723821019$, which value is drawn as the horizontal dashed-line in Fig. 11.

For the second example, we consider the condenser $(\mathbb{D}, E)$ where E consists of four lens domains as in Fig. 12. Each of these lenses is defined by two circular arcs, each of which passes through three given points. The values of these points are given in Fig. 12(b). The computed value of the capacity is

$$\mathrm{cap}(\mathbb{D}, E) = 17.613666396960355. \tag{5.4}$$

Note that this value of the capacity is close to the value of the capacity of the annulus $0.7 < |z| < 1$ which is 17.615998583457760.

6. Conclusion

Polycircular domains are domains whose boundaries are unions of arcs of circles and rectilinear segments. Computation of conformal capacity of such domains in closed form is possible only in simple geometric configurations, and numerical

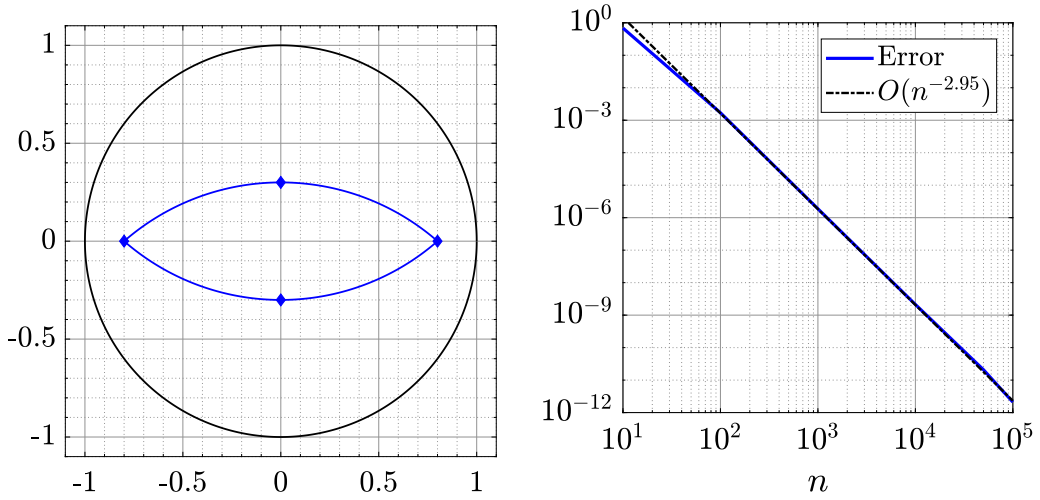

(a) The domain $\mathbb{D}\backslash E$ for the lens E. (b) Convergence of BIE.

Fig. 10. Lens domain with $r = 4/5$, $s = 3/10$. The reference value is 10.15585205509004.

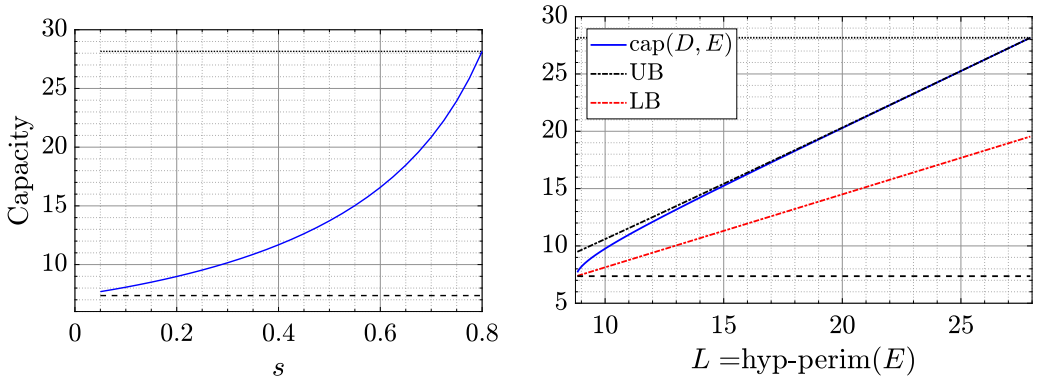

(a) Capacity as function of s. (b) Capacity as function of hyperbolic perimeter.

Fig. 11. The capacity cap$(\mathbb{D}, E)$, the upper bound (5.1), and the lower bound (5.2) where E is the lens domain with $r = 0.8$ and $0 < s \leq r$ vs. the hyperbolic perimeter of E. The horizontal dot line is cap$(\mathbb{D}, \overline{B(0, r)})$ and the horizontal dashed line is cap$(\mathbb{D}, [-r, r])$.

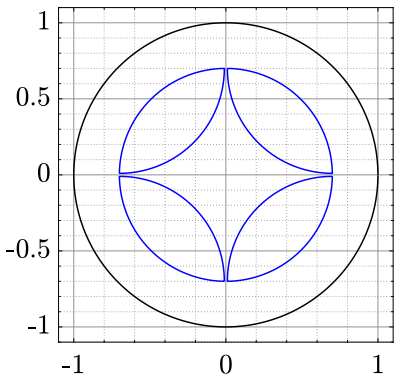

(a) The domain.

Lens 1	Arc 1	Arc 2
Point 1	$0.01 + 0.7\mathrm{i}$	$0.7 + 0.01\mathrm{i}$
Point 2	$0.7(1 + \mathrm{i})/\sqrt{2}$	$0.3(1 + \mathrm{i})/\sqrt{2}$
Point 3	$0.7 + 0.01\mathrm{i}$	$0.01 + 0.7\mathrm{i}$

(b) Single lens configuration.

Fig. 12. The domain $\mathbb{D}\backslash E$ where E consists of four lenses. The four lenses are defined as rotated images of the configuration given in (b).

approximations are necessary. As always with approximations, the central question is the accuracy of the obtained results. Within the PDE context the existing methods such as *hp*-FEM are equipped with error estimators, that can be shown to be asymptotically correct. Here we employ another approach for verification — we apply two different numerical methods, *hp*-FEM and the boundary integral method, with different discretization characteristics. Theoretical error bounds are not yet available in the case of the method based on the BIE with the generalized Neumann kernel. On the other hand, the BIE method has turned out to be very flexible and easily adjustable to great many geometries with high precision in the cases reported in [8,9]. The numerical experiments presented in this paper gave further evidence about the accuracy of this BIE method and illustrate that the BIE method gives results with a comparable level of accuracy with the *hp*-FEM. Furthermore, the BIE method is not only easier to implement but also consistently faster both in terms of problem setup and solution time within the class of problems considered here. For an example implementation, we refer to https://github.com/mmsnasser/polycircular.

Over a carefully designed set of numerical experiments we first establish the convergence properties of the methods, then verify the agreement against known reference results, and finally compare the results. The computed capacities are extremely accurate and can serve as reference values. In some cases even practical machine precision is obtained. More importantly, in those cases where the results differ, though never over the single precision, the discrepancy between the methods is within the asymptotic error estimates. This gives us very high confidence that the numbers reported here are indeed as accurate as we claim.

In conclusion, we have used two methods to compute capacity of condensers which requires solving a Dirichlet boundary value problem in multiply connected domains for the harmonic potential function whose values are equal to zero on the outer boundary component and equal to one on all inner boundary components. The presented methods can be used to compute other quantities in potential theory which require computing harmonic functions with other type of boundary conditions, see [8,50]. For example, recently, an analytic formula for computing a quantity known as the "h-function" for multiply connected slit domains is presented in [51]. The numerical computation of the "h-function" for multiply connected slit domains can be formulated as a boundary value problem of the type considered in [8] and hence the *h*-function can be computed for multiply connected domains with high connectivity by the BIE method.

Acknowledgments

The authors would like to thank two anonymous reviewers for their valuable comments and suggestions which greatly improved the presentation of this paper.

References

[1] D. Crowdy, Solving problems in multiply connected domains. CBMS-NSF regional conference series in applied mathematics, in: Society for Industrial and Applied Mathematics (SIAM), Philadelphia, PA, vol. 97, 2020, p. 434, ©2020.
[2] L.V. Ahlfors, Conformal invariants: topics in geometric function theory, in: McGraw-Hill Series in Higher Mathematics, McGraw-Hill Book Co, New York-Düsseldorf-Johannesburg, 1973, p. ix+157.
[3] V.N. Dubinin, Condenser Capacities and Symmetrization in Geometric Function Theory, Birkhäuser, 2014.
[4] D.F. Abzalilov, P.N. Ivanshin, E.A. Shirokova, Solution the Dirichlet problem for multiply connected domain using numerical conformal mapping, Complex Anal. Oper. Theory 13 (3) (2019) 1419–1429.
[5] G. Pólya, G. Szegö, Isoperimetric inequalities in mathematical physics, in: Annals of Mathematics Studies, vol. 27, Princeton University Press, Princeton, N. J, 1951, p. xvi+279.
[6] J.B. Garnett, D.E. Marshall, Harmonic Measure, Cambridge University Press, Cambridge, 2008.
[7] M.M.S. Nasser, O. Rainio, A. Rasila, M. Vuorinen, T. Wallace, H. Yu, X. Zhang, Circular arc polygons, numerical conformal mappings, and moduli of quadrilaterals, Adv. Comput. Math. 48 (58) (2022) arXiv:2107.11485 [math.CV], p. 28.
[8] M.M.S. Nasser, M. Vuorinen, Numerical computation of the capacity of generalized condensers, J. Comput. Appl. Math. 377 (2020) 112865.
[9] M.M.S. Nasser, M. Vuorinen, Computation of conformal invariants, Appl. Math. Comput. 389 (2021) 125617.
[10] R. Kühnau, Canonical conformal and quasiconformal mappings. Identities. Kernel functions, in: Handbook of Complex Analysis: Geometric Function Theory, vol. 2, Elsevier Sci. B. V, Amsterdam, 2005, pp. 131–163.
[11] N. Papamichael, N. Stylianopoulos, Numerical Conformal Mapping: Domain Decomposition and the Mapping of Quadrilaterals, World Scientific Publishing Co. Pte. Ltd, Hackensack, NJ, 2010, p. xii+229.
[12] P.K. Kythe, Handbook of Conformal Mappings and Applications, CRC Press, Boca Raton, FL, 2019, p. xxxv+906.
[13] R. Wegmann, Methods for numerical conformal mapping, in: R. Kühnau (Ed.), Handbook of Complex Analysis: Geometric Function Theory, vol. 2, Elsevier B. V, 2005, pp. 351–477.
[14] P.R. Brown, R.M. Porter, Numerical conformal mapping to one-tooth gear-shaped domains and applications, Comput. Methods Funct. Theory 16 (2) (2016) 319–345.
[15] R.M. Porter, On the art of calculating accessory parameters of conformal mappings of circular arc polygons–general considerations and special situations, in: Teichmüller Theory and Moduli Problem, in: Ramanujan Math. Soc. Lect. Notes Ser, 10, Ramanujan Math. Soc., Mysore, 2010, pp. 549–576.
[16] U. Bauer, W. Lauf, Conformal mapping onto a doubly connected circular arc polygonal domain, Comput. Methods Funct. Theory 19 (1) (2019) 77–96.
[17] D.G. Crowdy, A.S. Fokas, Conformal mappings to a doubly connected polycircular arc domain, Proc. Roy. Soc. A 463 (2007) 1885–1907.
[18] P. Bjørstad, E. Grosse, Conformal mapping of circular arc polygons, SIAM J. Sci. Stat. Comput. 8 (1987) 19–32.
[19] L.H. Howell, Numerical conformal mapping of circular arc polygons, J. Comput. Appl. Math. 46 (1993) 7–28.
[20] L.N. Trefethen, Numerical conformal mapping with rational functions, Comput. Methods Funct. Theory 20 (2020) 369–387.
[21] D.G. Crowdy, A.S. Fokas, C.C. Green, Conformal mappings to multiply connected polycircular arc domains, Comp. Meth. Funct. Theory 11 (2) (2011) 685–706.
[22] S. Bergman, The kernel function and conformal mapping, Amer. Math. Soc. (1970).

[23] G.M. Goluzin, Geometric theory of functions of a complex variable, Amer. Math. Soc. (1969).
[24] P. Koebe, Abhandlungen zur Theorie der konformen Abbildung, IV. Abbildung mehrfach zusammenhängender schlichter Bereiche auf Schlitzbereiche, Acta Math. 41 (1918) 305–344.
[25] Z. Nehari, Conformal Mapping, Dover Publications, New York, 1952.
[26] M. Tsuji, Potential Theory in Modern Function Theory, Chelsea Publishing Co, New York, 1975.
[27] M. Badreddine, T.K. DeLillo, S. Sahraei, A comparison of some numerical conformal mapping methods for simply and multiply connected domains, Discrete Contin. Dyn. Syst. Ser. B 24 (1) (2019) 55–82.
[28] E. Kropf, X. Yin, S.-T. Yau, X. Gu, D. Xianfeng, Conformal parameterization for multiply connected domains: combining finite elements and complex analysis, Eng. Comput. 30 (4) 441–455, http://dx.doi.org/10.1007/s00366-013-0348-4.
[29] M.M.S. Nasser, Numerical conformal mapping via a boundary integral equation with the generalized Neumann kernel, SIAM J. Sci. Comput. 31 (2009) 1695–1715.
[30] M.M.S. Nasser, PlgCirMap: A MATLAB toolbox for computing the conformal mapping from polygonal multiply connected domains onto circular domains, SoftwareX 11 (2020) 100464, arXiv 2019, arXiv:1911.01787.
[31] L. Greengard, Z. Gimbutas, FMMLIB2D: A MATLAB toolbox for fast multipole method in two dimensions, 2019, version 1.2 http://www.cims.nyu.edu/cmcl/fmm2dlib/fmm2dlib.html. (Accessed 6 2020).
[32] M.M.S. Nasser, O. Rainio, M. Vuorinen, Condenser capacity and hyperbolic perimeter, Comput. Math. Appl. (2022) 54–74.
[33] H. Hakula, A. Rasila, M. Vuorinen, On moduli of rings and quadrilaterals: algorithms and experiments, SIAM J. Sci. Comput. 33 (2011) 1.
[34] H. Hakula, A. Rasila, M. Vuorinen, Computation of exterior moduli of quadrilaterals, Electron. Trans. Numer. Anal. (ISSN: 1068-9613) 40 (2013) 1–16.
[35] M.M.S. Nasser, Fast solution of boundary integral equations with the generalized Neumann kernel, Electron. Trans. Numer. Anal. 44 (2015) 189–229.
[36] F.W. Gehring, G.J. Martin, B.P. Palka, An introduction to the theory of higher-dimensional quasiconformal mappings, in: Mathematical Surveys and Monographs, vol. 216, American Mathematical Society, Providence, RI, 2017, p. ix+430.
[37] P. Hariri, R. Klén, M. Vuorinen, Conformally invariant metrics and quasiconformal mappings, in: Springer Monographs in Mathematics, Springer, Berlin, 2020.
[38] I. Babuška, M. Suri, The P and H-P versions of the finite element method, basic principles and properties, SIAM Rev. 36 (1994) 578–632.
[39] Ch. Schwab, *p*- and *hp*-Finite Element Methods, Oxford University Press, 1998.
[40] H. Hakula, T. Tuominen, Mathematica implementation of the high order finite element method applied to eigenproblems, Computing 95 (2013) 277–301.
[41] H. Hakula, M. Neilan, J. Ovall, A posteriori estimates using auxiliary subspace techniques, J. Sci. Comput. 72 (1) (2017) 97–127.
[42] I. Babuška, B. Guo, Regularity of the solutions of elliptic problems with piecewise analytical data, parts I and II, SIAM J. Math. Anal. 19 (1988) 172–203 and 20, (1989) 763–781.
[43] F.D. Gakhov, Boundary Value Problems, Pergamon Press, Oxford, 1966.
[44] S.G. Mikhlin, Integral Equations and their Applications To Certain Problems in Mechanics, Mathematical Physics and Technology, second ed., Pergamon Press, Oxford, 1964.
[45] R. Kress, A Nyström method for boundary integral equations in domains with corners, Numer. Math. 58 (2) (1990) 145–161.
[46] K.E. Atkinson, The numerical solution of integral equations of the second kind, Cambridge University Press, Cambridge, 1997.
[47] R. Kress, Boundary integral equations in time-harmonic acoustic scattering, Math. Comput. Modelling 15 (1991) 229–243.
[48] J. Liesen, O. Séte, M.M.S. Nasser, Fast and accurate computation of the logarithmic capacity of compact sets, Comput. Methods Funct. Theory 17 (2017) 689–713.
[49] R. Wegmann, M.M.S. Nasser, The Riemann-Hilbert problem and the generalized Neumann kernel on multiply connected regions, J. Comput. Appl. Math. 214 (2008) 36–57.
[50] H. Hakula, Adaptive reference elements via harmonic extensions and associated inner modes, Comput. Math. Appl. 80 (11) (2020) 2272–2288.
[51] C.C. Green, M.A. Snipes, L.A. Ward, D.G. Crowdy, Harmonic-measure distribution functions for a class of multiply connected symmetrical slit domains, Proc. Roy. Soc. A 478 (2022).